POLYSACCHARIDE-REDUCED AND CAPPED GOLD NANOPARTICLES FOR ANTIMICROBIAL AND PHOTOCATALYTIC APPLICATIONS

AAMNA MAJEED,[*] RASHIDA BASHIR,[**] BEHRAM SHAHZAD,[*] MUHAMMAD UMAIR SHARIF,[*] GULZAR MUHAMMAD,[*] MUHAMMAD ARSHAD RAZA,[*] MUHAMMAD WAJID,[***] TUBA TUBA[****] and ALINA SIONKOWSKA[****,*****]

[*]*Department of Chemistry, Institute of Chemical Sciences, Government College University Lahore, 54000 Lahore, Pakistan*
[**]*Division of Science and Technology, University of Education Lahore, Pakistan*
[***]*Habib Institute of Health Sciences, Mian Channu, The Islamia University of Bahawalpur, Bahawalpur, Pakistan*
[****]*Laboratory for Biomaterials and Cosmetics, Faculty of Chemistry, Institute of Advanced Studies, Nicolaus Copernicus University in Toruń, Poland*
[*****]*Faculty of Medicine and Health Sciences, University of Kalisz, Poland*
✉ *Corresponding authors: G. Muhammad, mgulzar@gcu.edu.pk*
A. Sionkowska, as@chem.umk.pl

Received March 29, 2026

This research investigates the green synthesis of gold nanoparticles (Au NPs) using a biodegradable and natural reducing agent, arabinoxylan mucilage from *Plantago major* seeds. UV-Vis spectroscopy revealed a characteristic surface plasmon resonance peak at 550 nm, with an energy band gap of 3.45 eV, confirming Au NP formation. FTIR analysis revealed peaks corresponding to alcohol, carbonyl, and other functional groups, along with a distinct metal-oxygen bond signal, demonstrating the participation of the groups in NP stabilization. SEM revealed globular-shaped particles (78 nm), while EDX analysis confirmed the elemental composition. XRD patterns verified the crystalline NPs with a face-centered cubic structure. The Au NPs exhibited effective microbicidal potential against *Escherichia coli* (ZOI 25 ± 0.66 mm), *Bacillus cereus* (ZOI 18 ± 0.33 mm), and *Enterobacter aerogenes* (ZOI 11 ± 0.98 mm). The significant minimum inhibitory and bactericidal concentrations (MICs and MBCs) were investigated for bacterial strains, confirming the antimicrobial potential of Au NPs. Furthermore, the Au NPs demonstrated remarkable photocatalytic performance with degradation efficiencies of 89% for methylene blue (MB) and 81.19% for methyl orange (MO) under pseudo-first-order kinetics, highlighting their potential for wastewater treatment.

Keywords: *Plantago major*, arabinoxylan, mucilage, gold nanoparticles, photocatalytic

INTRODUCTION

Nanomaterials synthesized from plant materials possess the advantage of adjustments in structure, surface area, morphology, and size that can be achieved through experimental conditions and the choice of precursors.[1] Like other nanomaterials, Au NPs are highly chemically stable,[2] widely utilized in biomedical applications, such as the detection of molecules, cancer phototherapy, drug delivery, and biosensing.[3] Au NPs are used for biological, catalytic, and environmental applications due to their electronic, physicochemical, and optical characteristics.[4] Au NPs have a large surface area, smaller sizes, adjustable surface functions, and plasma resonance properties that affect their stability and functionality for several biomedical and environmental remediation applications.[5]

Physical and chemical methods for producing NPs involve toxic chemicals, such as a reducing agent, yield harmful by-products, and require further purification.[6] Green route synthesis overcomes such limitations using biomolecules from plant precursors.[7] Biological activities of Au NPs are not only improved using a green synthesis approach, but also influenced in terms of physical and chemical properties, such as particle size, shape, accumulation, surface modifications, and concentration of NPs.[8] Green-synthesized NPs exhibited more surface functionalization due to the binding of more phytochemicals from plant materials, which increased stability and biological activities.[9]

Various plant materials (extracts and mucilages) utilized for reducing and stabilizing NPs[10] as natural alternatives to synthetic polymers[11] represent sustainable products.[12] Mucilages extracted from seeds

have a branched polysaccharide structure, containing galacturonic acid, *D*-galactose, *L*-arabinose, and *D*-xylose, with phenolic contents,[13] being biodegradable,[14] renewable and sustainable,[15] functionally bioactive, and cost-effective materials.[16] They can be used in drug delivery,[17] tissue engineering[18] contact lenses,[19] agricultural and horticultural applications,[20] cosmetics and personal care products,[21] food industry for packaging, or texturing component,[22] electronics,[23] biosensing and diagnostic applications,[24] environmental remediation[25] and reducing metal ions to NPs.[26]

Arabinoxylan-rich mucilage from *P. major* seeds consists of monosaccharides, such as arabinose, xylose, galacturonic acid, glucose, and rhamnose, along with other sugars, and has diverse applications.[27] The mucilage offers sustained drug delivery because it works as a drug-binding agent, while controlling drug release patterns.[28] Such mucilage is effective for wound healing due to its water retention capacity and gelling properties that develop a humid environment near the affected area and enhance tissue regeneration, wound resurfacing, and cell transfer for wound recovery.[29] Additionally, *P. major* also possesses anti-inflammatory properties that decrease inflammation and promote tissue regeneration, which is significant for wound healing.[30] The cosmetic sector uses it for face masks, as well as conditioners and moisturizers.[31] Mucilage is also a promising candidate in wastewater treatment, water filtration systems, and for the synthesis of biodegradable polymeric products due to its water-absorbing and gelling properties. The mucilage shows potential for food processing and the development of dietary supplements with thickening and stabilizing properties, being used as texturing, gelling and thickening agent.[32] *P. major* mucilage enhances fabric fibers and their texture strength in textile production to produce biodegradable fabrics, replacing typically used synthetic textile additives. In agriculture, *P. major* mucilage functions as protective soil insulation for improved farm yields, pesticide protection, a bio-stimulant to bolster plant germination and root development, and has antimicrobial properties that protect plants from fungal and bacterial pathogens.[33,34]

Direct discharge of textile wastewater containing dyes and other pollutants without proper disposal causes water pollution, with serious consequences for ecosystems.[35] This not only contaminates drinking water resources, but also severely affects water bodies and wildlife through toxic chemicals, exhibiting severe effects, even with low concentrations of these pollutants.[36] Textile dyes, including MO and MB, are carcinogenic and are widely used in products across textiles, pharmaceutical, food, cosmetics, and agricultural sectors for various purposes.[37] Both MO and MB can cause health issues, including vomiting, diarrhea, skin infections, eye damage, and cyanosis. Still, MB causes more harmful effects than MO (anionic dye) because of its cationic nature.[38] Different methods were used to remove dyes from wastewater, including photocatalytic destruction, osmosis, flotation, ion exchange, chlorination, adsorption, and electrochemical transformation; however, these methods required more complex apparatus with less significant removal efficiency. Photocatalytic dye degradation through green-synthesized NPs is not only a cost-effective and eco-friendly approach for dye removal, but also provides reusability with effective removal.[39]

A few studies are available on *P. major* seed mucilage and the evaluation of its reduction and stabilizing potential for metal ions to NPs. The present study approaches the eco-friendly, sustainable, and cost-effective synthesis of Au NPs from the arabinoxylan-rich mucilage of *P. major* seeds. The NPs were characterized through UV-Vis spectroscopy, FTIR, SEM, EDX, and XRD to confirm the formation, structure, morphology, chemical composition, and size. Various uses of Au NPs for biomedical and environmental applications were evaluated through antibacterial activity and photocatalytic degradation of textile dyes for wastewater treatment.

EXPERIMENTAL

Materials

Gold chloride ($AuCl_3$) (99% purity), methylene blue ($C_{16}H_{18}ClN_3S$) (Dye content, ≥82%), and methyl orange ($C_{14}H_{14}N_3NaO_3S$) (Dye content, 85%) were purchased from Merck (Sigma-Aldrich). *P. major* seeds were procured from a local market and confirmed by a botanist at the Government College University Lahore, using a voucher specimen (GC. Herb. Bot. 4382), as being *P. major* Linn., of *Plantaginaceae* family. Bacterial strains (*E. coli*, *B. cereus*, and *E. aerogenes*) were acquired from the Microbiology Laboratory, Government College University Lahore.

Mucilage extraction

The hot water extraction method was used for mucilage extraction. For this purpose, washed and cleaned seeds were mixed with deionized hot water (70 °C, 90 min). When seeds extruded mucilage, the extracted mucilage was

separated from the seeds by a cloth before drying at 80 °C. The fine, dried powder of seed mucilage was stored carefully for further use.

Au NPs synthesis

A gold chloride ($AuCl_3$) suspension (20 mM) and a 1.0% suspension of seed mucilage were prepared by adding $AuCl_3$ (0.06 g) and mucilage (0.1 g) in deionized water (10 mL) separately. Both suspensions were mixed and stirred (2 h, 60 °C) until the color of the mixture changed to purple, demonstrating the formation of Au NPs. The Au NPs mixture was then centrifuged (20 min at 4500 rpm) to purify by eliminating non-reacted gold ions, excessive organic compounds, and mucilage residue. The purified Au NPs were washed with deionized water and ethanol and subjected to drying at 60 °C. Au NPs in powder form were characterized using spectroscopic techniques and stored carefully for further biological applications.

Characterization

The freshly prepared Au NPs suspension was characterized using a UV-Vis spectrophotometer (Agilent Cary 60) to verify the NPs synthesis. The Tauc relation was used to calculate the energy band gap (E_g) of Au NPs using Equation 1:

$$(\alpha h\nu)^m = A(h\nu - E_g) \quad (1)$$

The absorption coefficient (α) calculated from the UV-Vis spectrum was plotted as $(\alpha h\nu)^m$ vs photon energy (hν), where m indicates the character of the electronic transition.[40]

Dried, finely ground powder of Au NPs was used for FTIR analysis using an FTIR spectrophotometer (Agilent Cary 630). For SEM (Nova Nano SEM 450) and EDX with SEM at 10 kV analysis, dried NPs were placed on the aluminium stub using double-sided carbon tape and a thin layer of gold (as needed) to make the sample conductive. The micrographs were captured at different magnifications to observe particle shape, aggregation, and approximate size distribution. Calcined (450 °C, 3 h) and desiccated Au NPs were used for XRD analysis by an X-ray diffractometer (Proto AXRD LPD) to enhance crystallinity and peak diffraction. Dried NP powder was deposited as thin films on glass substrates, and diffraction patterns were observed over a suitable 2θ range (10-80°) in Cu Kα radiation.

Antibacterial activity

The antimicrobial potential of Ag NPs against the three above-mentioned bacterial strains (*E. coli*, *E. aerogenes*, and *B. cereus*) was evaluated using the agar well diffusion method. Pre-inocula of pathogen strains were prepared and adjusted according to a 0.5 McFarland turbidity standard and spread on Mueller-Hinton agar plates using a sterile cotton swab. Five agar wells (6.0 mm diameter) were completed on each agar plate using a sterile cork borer. NP sprays were obtained in ethanol-water (1:1, V/V) to achieve final concentrations of 100, 50, and 25 µg/mL. The concentration (100 µL) was transferred to different wells with care. The positive control was rifampicin (50 µg/mL), and the negative control was ethanol-water (1:1) without NPs. Each plate was incubated at 37 °C for 24 h. During incubation, clear zones of inhibition (ZOI) around the wells were measured with a digital caliper in millimeters. All assays were performed in triplicate for each NP type and concentration, and the mean ±SD was calculated.

MIC and MBC determination

MIC is the minimum concentration of Au NPs that prevents microbial growth, and MBC refers to the concentration of Au NPs to kill 99.9% of the initial microbial inoculum. MIC values were determined for the prepared Au NPs using 24-h-old cultures (*E. coli*, *B. cereus*, and *E. aerogenes*) suspended in nutrient broth (3 mL in each test tube) for incubation (37 °C, 24 h). Bacterial culture (30 µL) adjusted to a 0.5 McFarland turbidity standard was added to tubes containing fresh nutrient broth (3 mL), supplemented with varying concentrations (5, 10, 15, 20, 25, and 30 µg mL^{-1}) of the prepared compound. After an overnight incubation period (37 °C), optical density (OD) was measured at 523 nm using a spectrophotometer. The test tube with no increase in OD was taken as MIC. To find MBC, MIC (100 µL) with a lower OD was placed on nutrient agar plates before incubation (37 °C, 24 h).

After MIC determination, freshly prepared nutrient broth (3.0 mL) was mixed in a sterile test tube and then mixed with the bacterial culture (30 µL). The serial concentrations of Au NPs (30-180 µL mL^{-1}) were mixed in all test tubes, except the negative control. After incubation (37 °C, 24 h), the OD was calculated at 523 nm. MBCs were determined by incubation for 24 h at 37 °C after spreading MICs (100 µL) on nutrient agar plates.

Photocatalytic activity

The potential of Au NPs for degrading textile dyes was evaluated using MB and MO dyes. Solutions with varying concentrations (5-10 mg/100 mL) for both dyes were diluted to 10 ppm (50 mL). The diluted dye solution was stirred with Au NPs (1.0-5.0 mg) for 150 min in sunlight for photocatalytic degradation. A pure sample of dye was taken before adding NPs as a baseline for comparison of degradation extent. Approximately 10 mL of each

sample was drawn at regular 30-minute intervals to assess the maximum degradation effectiveness. Samples were exposed to UV-vis analysis, scanned in the UV-visible range of 700-300 nm to explore degradation efficiency using Equation (2):

$$\% \text{ Dye degradtion} = \frac{C_0 - C_t}{C_t} \quad (2)$$

where C_0 and C_t are the initial and final dye concentrations before and after adding NPs. The following Equation (3) assesses kinetics:

$$\text{In } \frac{C_t}{C_0} = -KT \quad (3)$$

where C_0 and C_t are dye concentrations at zero time and after treatment with NPs at time t, and k is the rate constant for the reaction.

RESULTS AND DISCUSSION

Characterization

The synthesized Au NPs were characterized using spectroscopic techniques (UV-Visible, FTIR, SEM, EDX, and XRD) to confirm formation, morphology, elemental composition, and crystalline structure of NPs.

UV-Visible spectroscopy

The UV-vis absorption spectrum of Au NPs (Fig. 1) exhibits a SPR band at about 550 nm (λ_{max}), confirming the successful formation of NPs through Au^{3+} ions reduction to metallic Au NPs. A typical feature of spherical Au NPs dispersed in an aqueous medium is the appearance of an SPR band ranging at 520-530 nm. A slight (red) shift to 550 nm for Au NPs in this study indicated more formation of NPs through reduction and stabilization of NPs by the mucilage. The absorption mechanism starts with the fall of photons of equal energy on the surface of NPs; they accelerate the oscillations of free conduction electrons via surface plasmons that induce absorption. The resonant potential of NPs is dependent on multiple factors, such as size, morphology, and composition of the NPs. UV-vis absorption wavelength is consistent with Au NPs prepared with the hydrogel from seeds of *Cydonia oblonga*.[41]

The linear portion of the Tauc plot was extrapolated to the energy axis, yielding a band gap of 3.45 eV (Fig. 2). The energy band gap value exhibited by Au NPs corresponds to the previously reported value (3.41 eV) for Au NPs prepared through a green method from a leaf extract of the *Wedelia trilobata* plant.[42] Differences in NP size, morphology, and the extent of surface functionalization by the capping biomolecules can be explained by minor changes in the band gap. The gap between the quantized gold bands is relatively large, suggesting strong quantum confinement at the nanoscale.

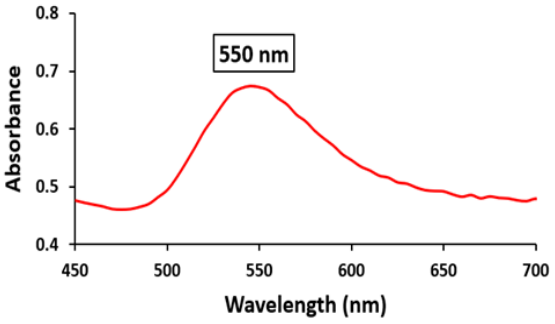

Figure 1: UV-Visible spectrum of Au NPs from *P. major* seed mucilage as reducing and capping agent

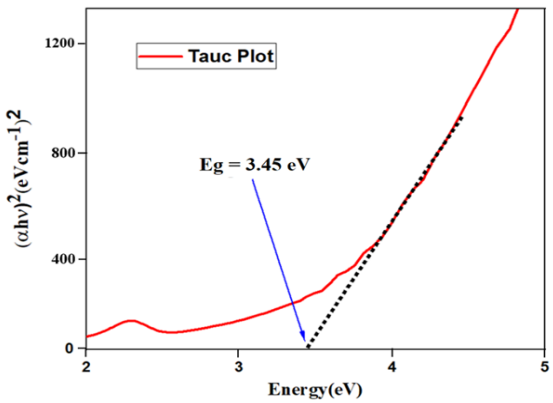

Figure 2: Energy band gap (eV) of the Au NPs from the Tauc plot

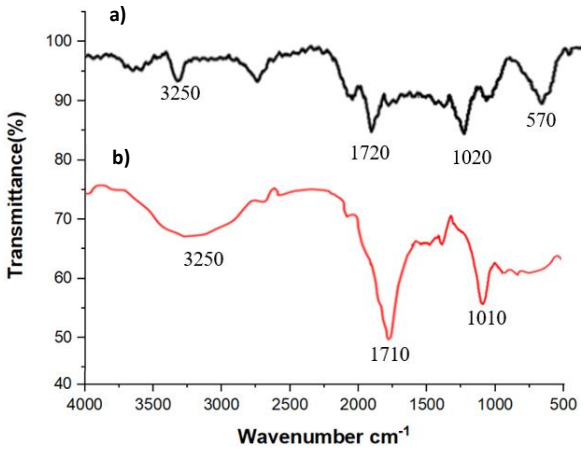

Figure 3: FTIR spectra with functional group peaks for Au NPs (a) and PM mucilage (b)

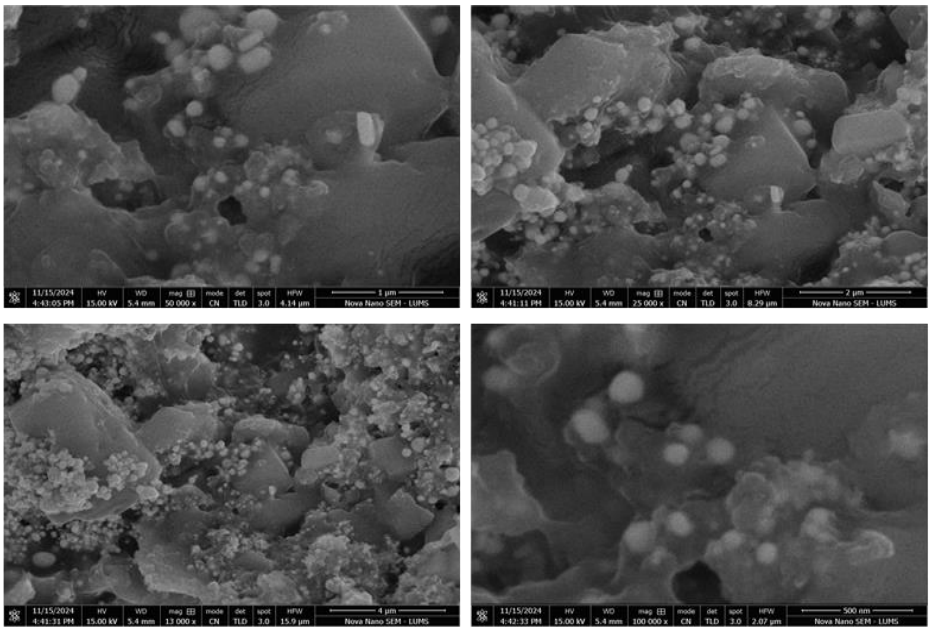
Figure 4: SEM images of Au NPs at different magnifications (1, 2, and 4 µm, and 500 nm)

FTIR analysis

The FTIR spectra of Au NPs and PM mucilage (Fig. 3) were recorded for both simple mucilage and dried, non-calcined NPs that retained biomolecules of mucilage adhered to the surface of NPs. Both spectra exhibited peaks corresponding to different functional groups, including hydroxyl and carboxyl, which reduced Au^{3+} ions to Au NPs.[43] The bands at 3250 cm^{-1} agreed with the O-H functional group present in the mucilage structure. The absorption band at 1710 cm^{-1} is due to the stretching of the carbonyl group, and C-O bond stretching peaks occur in the range of 1000-1300 cm^{-1}.[44] The increase in peak intensity of Au NPs compared to mucilage, with a new peak at 570 cm^{-1}, confirms that metal-oxygen interactions lead to the formation of Au NPs.[45]

SEM analysis

SEM analysis established the morphology of Au NPs at different magnifications (1, 2, and 4 µm, and 500 nm) (Fig. 4). SEM images describe the globular shape with orbicular clusters of NPs, agglomeration of homomorphic globular particles, and the macro-scale framework coincides with the mucilage polysaccharidal substances that reduce and stabilize NPs. The synthesized Au NPs were implanted in the mucilage matrix instead of being solely distributed, due to which particles remain enclosed in a polysaccharidal network.[46]

The average diameter of the NPs evaluated using ImageJ software was 78 nm. Similar morphology and sizes were observed for Au NPs synthesized from quince seed mucilage in the literature.[47]

EDX analysis

EDX analysis was conducted to evaluate the elemental composition of the synthesized Au NPs. The EDX spectrum (Fig. 5) of Au NPs reveals distinct indications of Au, C, O, Na, Mg, Si, Cl, K, and Fe. Carbon and oxygen in the EDX spectrum appeared from the mucilage on the surface of NPs. Metal ions other than gold in the EDX spectrum might be trace inorganic minerals in the mucilage capping the NPs. The appearance of silicon might be interfering from the glassware used during the EDX spectroscopy.[48] Therefore, EDX analysis exhibited a composition with a major gold constituent, while the formation of NPs was confirmed in conjunction with the UV-Vis, XRD, and SEM results.

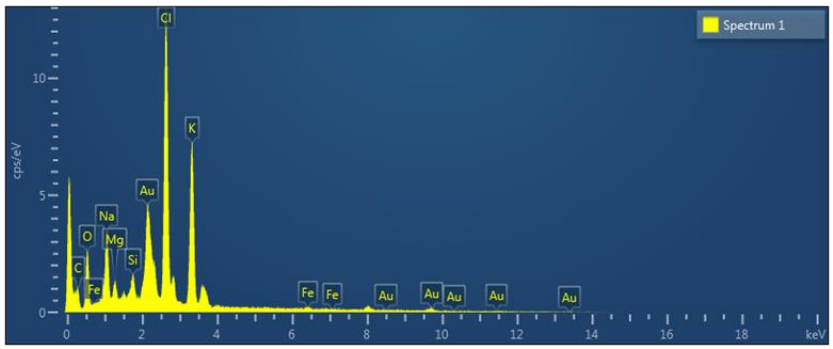

Figure 5: EDX spectrum of Au NPs

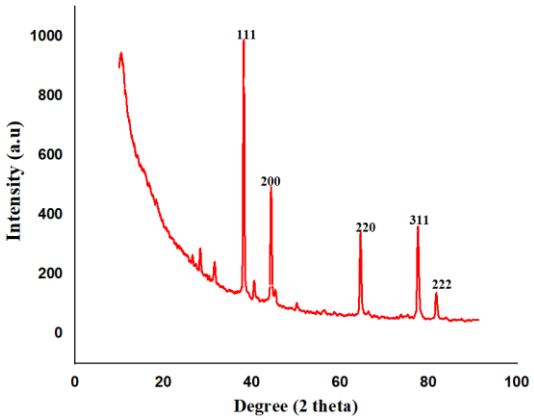

Figure 6: XRD diffraction of Au NPs with peak planes at 2θ angles

XRD analysis

The purity and crystal structure properties of the synthesized Au NPs were evaluated by XRD analysis. The XRD diffraction pattern in Figure 6 reveals the crystalline nature of Au NPs. specifically, the diffractogram indicates the presence of several peaks, which are attributed to the face-centered cubic structure of Au NPs. At angles of approximately 38.6, 44.4, 76.8, and 81.8° (exact indexing is dependent on the calibration of the instrument used), reflections corresponding to planes (111), (200), (220), (311), and (222) are observed compared to their standard JCPDS files (ICDD/JCPDS PDF Card No. 04-0784). The occurrence of these typical fcc reflections ascertains that the cores of the biosynthesized NPs are crystalline Au. Other weak peaks may result from residual organic constituents of the mucilage or small crystalline impurities. The XRD pattern shows that the green approach yields well-crystallized Au NPs, similar to those obtained via less conventional synthesis pathways.[49]

Antibacterial activity

For the investigation of the antibacterial activity of Au NPs, three pathogenic strains were used (*E. coli*, *E. aerogenes*, and *B. cereus*) (Fig. 7). Au NPs showed maximum inhibition activity against *E. coli*. Au NPs revealed ZOI with values of 25 ± 0.66, 18 ± 0.33, and 11 ± 0.98 mm against *E. coli*, *B. cereus*, and *E. aerogenes*, respectively. Thus, Au NPs are more effective against Gram-negative bacteria. This is in agreement with other findings from the literature for Au NPs formed from Melbury leaf extract,

which were also active against Gram-negative bacteria.[50] Similarly, Au NPs formed by *C. oblonga* seed hydrogel exhibited higher antibacterial potential against Gram-negative bacterial species, as it provided the maximum ZOI (18 nm) against *E. coli* bacterial strains.[41]

Also, the results indicated that *E. coli* had an MIC of 5.0 and an MBC of 10; *B. cereus* had an MIC and MBC of around 10; and *E. aerogenes* had the lowest MIC/MBC of 5.0 (mg mL^{-1}), indicating that it is the most resistant strain. Differences between species may be associated with variations in cell wall structure, membrane composition, and intrinsic defense mechanisms.

Green route-synthesized Au NPs exhibit higher antibacterial activity against bacterial strains for which chemically prepared Au NPs do not show significant activity. The potential of Au NPs may arise from using plant parts as precursors for the reduction of NPs, thereby enhancing their inhibition potential. This is particularly evident for different bacterial strains using plant extracts that have significant antibacterial activity.[51]

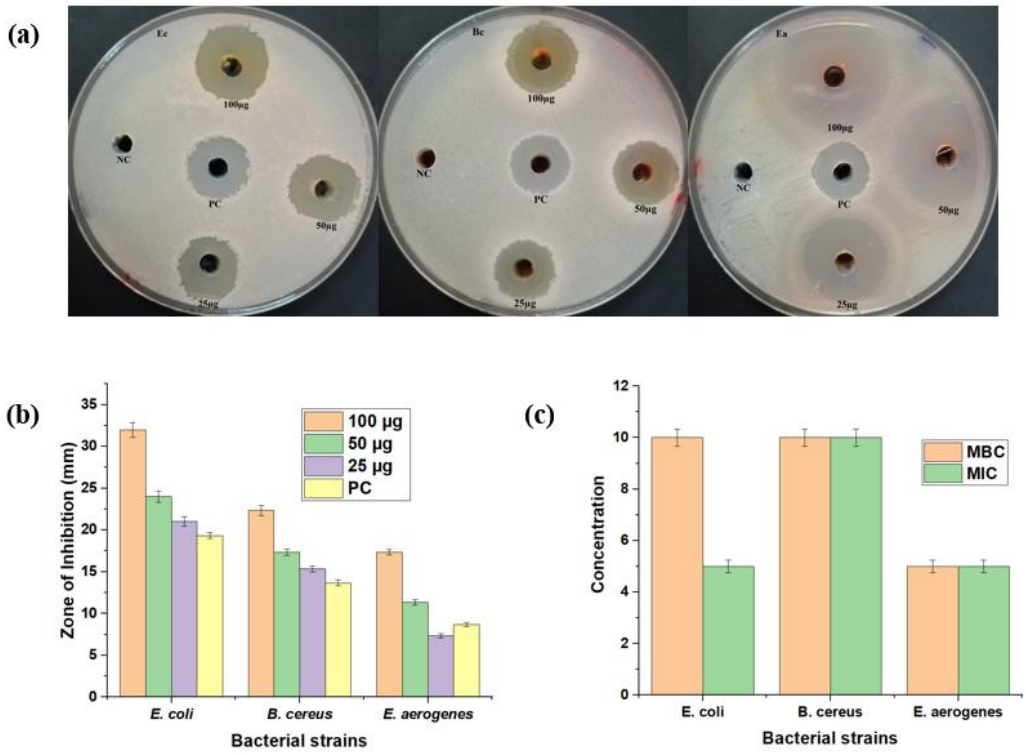

Figure 7: Antimicrobial potential of Ag NPs against three pathogen strains (a) *E. coli*, *B. cereus*, and *E. aerogenes*, (b) zones of inhibition against different bacteria, and (c) MBC and MIC values

Photocatalytic dye degradation

The dye degradation potential of Au NPs against MB and MO dyes was evaluated by measuring absorbance spectra. The color changes are shown in Figure 8. The absorption spectra of MB and MO (Fig. 9) indicate the reduction in the concentration of dyes over time. The peak intensity decreases with increasing reaction time, indicating the degradation of dyes by Au NPs. The colors of the dyes had almost disappeared after a 150-minute reaction in sunlight with NPs.

The maximum degradation of MB and MO was 89% and 81.19%, respectively, using optimized conditions of NP dosage (5 mg), dye concentration (50 mL), and sunlight exposure (150 min). The absorption of light by NPs produces charged species (positively charged) due to the excitation of electrons. The interaction of these charged species with water molecules generates hydroxyl radicals by oxidation, and conduction band electrons interact with molecular oxygen to generate superoxide anions.[52] These anions cause the degradation of dyes and accelerate the degradation process.[53] MB exhibits a higher percentage degradation due to its cationic nature, which improves the dye adsorption on the oxide surface. Therefore, a higher dye concentration on the surface leads to more MB degradation than MO, an anionic dye.[54]

The literature revealed similar results for the degradation of MB and MO dyes by green-synthesized Au NPs. A higher degradation percentage was shown for MB (98.02%) than MO (89.91%) for Au NPs synthesized from macroalgae *Halimeda macroloba* extract.[55] Au NPs formed by a banana peel aqueous extract were used to degrade MO and MB.[56] Au NPs using the aqueous extracts of *Alpinia nigra* leaves degrade MO with 83.25% degradation.[57] Au NPs produced using orange peel waste led to a degradation percentage of 90% for MO dye.[58]

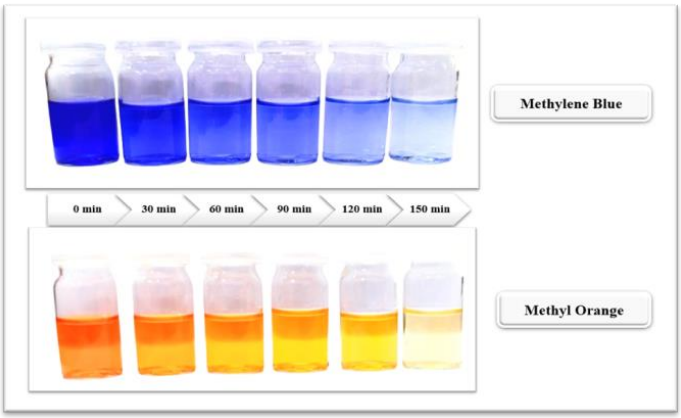

Figure 8: Color change of MB and MB dye solutions through photocatalytic degradation reaction for 150 min with Au NPs

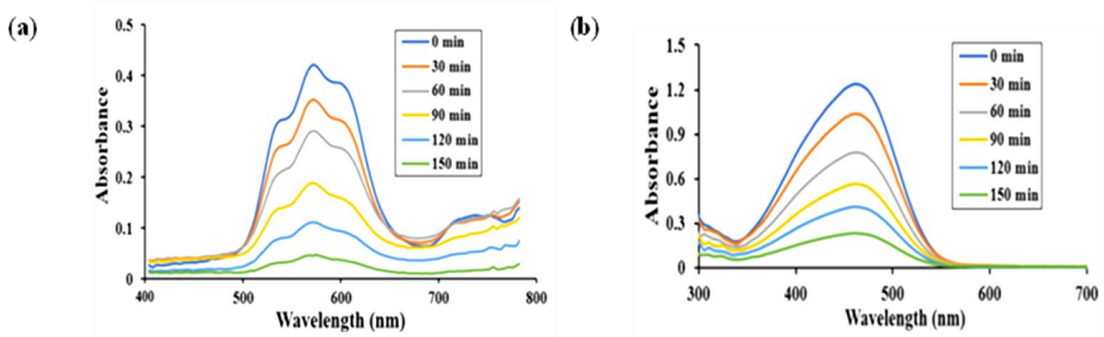

Figure 9: Absorption spectra of (a) MB and (b) MO dyes in contact with Au NPs over time

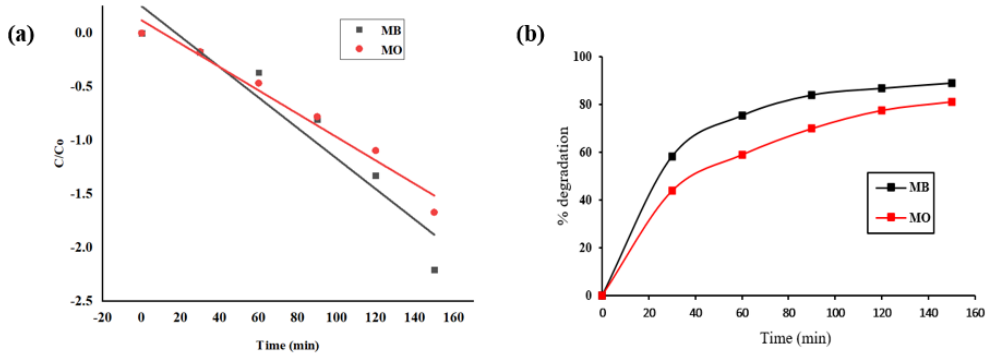

Figure 10: Kinetic plots (a) and degradation efficiency of MB and MO degradation (b) using Au NPs

Kinetic studies for the degradation of MB and MO dyes were assessed using the Langmuir-Hinshelwood model, which yields a linear relationship between time and ln (Co/C), as shown in Figure 10a. The kinetic plot confirms that the degradation reactions followed the pseudo-first-order kinetics, with rate constants (K) of -0.011/min (MO) and -0.014/min (MB), and with R^2>0.9 for MO (0.916) and MB (0.968). The degradation percentage of the dyes increases over time (Fig. 10b).

CONCLUSION

This study demonstrates the reduction potential of *P. major* seed mucilage, a natural biomaterial for the synthesis of Au NPs through a green route. These NPs were successfully characterized, confirming their formation, morphology, size, nature, and elemental composition by spectroscopic techniques. The antibacterial potential was also evaluated against three bacterial strains, and the results exhibited a significant growth inhibition capacity of Au NPs. Au NPs offer remarkable effectiveness for photocatalytic degradation of synthetic dyes, including MB and MO, in wastewater treatment processes.

This research presents an eco-friendly approach for synthesizing Au NPs that can be effectively used for environmental and biomedical applications. As a future perspective, by considering the antibacterial activity of AuNPs, their further antimicrobial-related applications can be evaluated. They could also be effective in food packaging because they can stop the growth of microorganisms and increase the shelf life of food products. However, more investigations are required to evaluate the efficiency and safety of Au NPs for biomedical applications, including drug preparation for fungal infection diseases. Moreover, different cytotoxic assays using cell lines and controls, and investigation mechanisms are demanded to demonstrate the biological safety of gold nanoparticles.

ACKNOWLEDGEMENT: Aamna Majeed acknowledges the Office of Research Innovation and Commercialization, Government College University Lahore (GCU-ORIC, No.224/ORIC/24) for funding her PhD research.

REFERENCES

[1] B. Mughal, S. Z. J. Zaidi, X. Zhang and S. U. Hassan, *Appl. Sci.*, **11**, 2598 (2021), https://doi.org/10.3390/app11062598

[2] S. Srivastava and A. Bhargava, in "Green Nanoparticles: The Future of Nanobiotechnology", Springer, Singapore, pp. 1–13 (2022), https://doi.org/10.1007/978-981-16-7106-7

[3] A. Hammami, N. M. Alabdallah, A. Al Jomaa and M. Kamoun, *J. King Saud Univ. Sci.*, **33**, 101560 (2021), https://doi.org/10.1016/j.jksus.2021.101560

[4] E. C. Dreaden, A. M. Alkilany, X. Huang, C. J. Murphy and M. A. El-Sayed, *Chem. Soc. Rev.*, **41**, 2740 (2012), https://doi.org/10.1039/C1CS15237H

[5] D. A. Giljohann, D. S. Seferos, W. L. Daniel, M. D. Massich, P. C. Patel *et al.*, *Angew. Chem. Int. Ed.*, **49**, 3280 (2010), https://doi.org/10.1002/anie.200904359

[6] S. Iravani, *Green Chem.*, **13**, 2638 (2011), https://doi.org/10.1039/C1GC15386B

[7] S. Ahmed, M. Ahmad, B. L. Swami and S. Ikram, *J. Adv. Res.*, **7**, 17 (2016), https://doi.org/10.1016/j.jare.2015.02.007

[8] A. Albanese, P. S. Tang and W. C. W. Chan, *Annu. Rev. Biomed. Eng.*, **14**, 1 (2012), https://doi.org/10.1146/annurev-bioeng-071811-150124

[9] A. E. Nel, L. Mädler, D. Velegol, T. Xia, E. M. V. Hoek *et al.*, *Nat. Mater.*, **8**, 543 (2009), https://doi.org/10.1038/nmat2442

[10] C. D. M. G. Martín, O. Ramírez, S. Bonardd, M. López-Darias, L. Franco *et al.*, *Int. J. Biol. Macromol.*, **268**, 131647 (2024), https://doi.org/10.1016/j.ijbiomac.2024.131647

[11] P. Anastas and N. Eghbali, *Chem. Soc. Rev.*, **39**, 301 (2010), https://doi.org/10.1039/B918763B

[12] R. Balart, D. Garcia-Garcia, V. Fombuena, L. Quiles-Carrillo and M. P. Arrieta, *Polymers*, **13**, 2532 (2021), https://doi.org/10.3390/polym13152532

[13] F. J. Barba, P. Putnik, D. B. Kovačević, M. M. Poojary, S. Roohinejad *et al.*, *Trends Food Sci. Technol.*, **67**, 260 (2017), https://doi.org/10.1016/j.tifs.2017.07.012

[14] A. Garcia-Garcia, S. Muñana-González, S. Lanceros-Mendez, L. Ruiz-Rubio, L. P. Alvarez *et al.*, *Polymers*, **16**, 2599 (2024), https://doi.org/10.3390/polym16182599

[15] B. A. Lodhi, M. A. Hussain, M. U. Ashraf, M. T. Haseeb, G. Muhammad *et al.*, *Ind. Crop. Prod.*, **155**, 112780 (2020), https://doi.org/10.1016/j.indcrop.2020.112780

[16] M. C. Catoira, L. Fusaro, D. Di Francesco, M. Ramella and F. Boccafoschi, *J. Mater. Sci.*: *Mater. Med.*, **30**, 115 (2019), https://doi.org/10.1007/s10856-019-6318-7

[17] A. Ali, M. A. Hussain, M. T. Haseeb, S. N. Bukhari *et al.*, *Curr. Drug Deliv.*, **20**, 292 (2023), https://doi.org/10.2174/1567201819666220509200019

[18] J. A. Hunt, R. Chen, T. van Veen and N. Bryan, *J. Mater. Chem. B*, **2**, 5319 (2014), https://doi.org/10.1039/C4TB00775A.

[19] X. Hu, L. Hao, H. Wang, X. Yang, G. Zhang *et al.*, *Int. J. Polym. Sci.*, **2011**, 814163 (2011), https://doi.org/10.1155/2011/814163

[20] Y. G. Maksimova, V. A. Shchetko and A. Yu. Maksimov, *Sel'skokhozyaistvennaya Biologiya*, **58**, 23 (2023), https://doi.org/10.15389/agrobiology.2023.1.23eng
[21] S. Mitura, A. Sionkowska and A. Jaiswal, *J. Mater. Sci.: Mater. Med.*, **31**, 50 (2020), https://doi.org/10.1007/s10856-020-06390-w
[22] H. Zhang, F. Zhang and R. Yuan, "Hydrogels Based on Natural Polymers", Elsevier, pp. 357–410 (2020), https://doi.org/10.1016/B978-0-12-816421-1.00015-X
[23] H. Omidian, S. D. Chowdhury and A. Akhzarmehr, *J. Bioact. Compat. Polym.*, **39**, 480 (2024), https://doi.org/10.1177/08839115241253260
[24] A. Herrmann, R. Haag and U. Schedler, *Adv. Healthcare Mater.*, **10**, 2100062 (2021), https://doi.org/10.1002/adhm.202100062
[25] G. Muhammad, K. N. Laila, M. U. Sharif, M. A. Hussain, A. Majeed *et al.*, *Cellulose Chem. Technol.*, **58**, 637 (2024), https://doi.org/10.35812/CelluloseChemTechnol.2024.58.58
[26] A. Majeed, G. Muhammad, M. R. Raza, M. Amin, A. Afzal *et al.*, *Cellulose Chem. Technol.*, **59**, 1033 (2025), https://doi.org/10.35812/CelluloseChemTechnol.2025.59.86
[27] B. Alizadeh Behbahani, F. Tabatabaei Yazdi, F. Shahidi, M. A. Hesarinejad, S. A. Mortazavi *et al.*, *Carbohyd. Polym.*, **155**, 68 (2017), https://doi.org/10.1016/j.carbpol.2016.08.051
[28] M. Saeedi, K. Morteza-Semnani and M. Sagheb-Doust, *Acta Pharm.*, **63**, 99 (2013), https://doi.org/10.2478/acph-2013-0010
[29] J. S. Boateng, K. H. Matthews, H. N. E. Stevens and G. M. Eccleston, *J. Pharm. Sci.*, **97**, 2892 (2008), https://doi.org/10.1002/jps.21210
[30] F. Jahanimoghadam, A. Javidan, M. Ranjbar, M. Torabi, S. Kakooei *et al.*, *BMC Complement. Med. Ther.*, **24**, 327 (2024), https://doi.org/10.1186/s12906-024-04621-z
[31] M. E. B. Rocha, L. Kakuda, E. B. Souto and W. P. Oliveira, *Sustain. Chem. Pharm.*, **42**, 101764 (2024), https://doi.org/10.1016/j.scp.2024.101764
[32] B. A. Behbahani, F. T. Yazdi, F. Shahidi, M. A. Hesarinejad, S. A. Mortazavi *et al.*, *Carbohyd. Polym.*, **155**, 68 (2017), https://doi.org/10.1016/j.carbpol.2016.08.051
[33] A. Nazarizadeh, P. Mikaili, M. Moloudizargari, S. Aghajanshakeri and S. Javaherypour, *J. Basic Appl. Sci. Res.*, **3**, 212 (2013)
[34] A. Majeed, S. Akram, G. Muhammad, M. R. Raza, R. Badar *et al.*, *J. Food Meas. Charact.*, **19**, 6470 (2025), https://doi.org/10.1007/s11694-025-03387-3
[35] R. Iriyadharsini, S. J. Jeyakumar and M. Jothibas, *Inorg. Chem. Commun.*, **154**, 110911 (2023), https://doi.org/10.1016/j.inoche.2023.110911
[36] M. Noor, M. Naseer, N. Arif, M. U. Sharif, T. Tuba *et al.*, *Cellulose Chem. Technol.*, **60**, 373 (2026), https://doi.org/10.35812/CelluloseChemTechnol.2026.60.31
[37] L. Wang, X. Qiang and Y. Song, *Mater. Today Sustain.*, **23**, 100435 (2023)
[38] C. Mao, H. Lei and Z. Guo, *Ceram. Int.*, **50**, 4737 (2024), https://doi.org/10.1016/j.ceramint.2023.11.218
[39] M. A. Hussain, A. Shaheen, S. Z. Hussain, I. Hussain, M. T. Haseeb *et al.*, *Cellulose Chem. Technol.*, **57**, 993 (2023), https://doi.org/10.35812/CelluloseChemTechnol.2023.57.87
[40] J. Peter, M. Backialakshmi, P. Karpagavinayagam and C. Vedhi, *J. Adv. Chem. Sci.*, **1**, 1 (2015)
[41] Z. Batool, G. Muhammad and M. M. Iqbal, *Sci. Rep.*, **12**, 6575 (2022), https://doi.org/10.1038/s41598-022-10495-3
[42] A. Dey, A. Yogamoorthy and S. M. Sundarapandian, *Res. J. Life Sci. Bioinform. Pharm. Chem. Sci.*, **4**, 1 (2018), https://doi.org/10.26479/2018.0406.01
[43] S. S. Shankar, A. Rai, A. Ahmad and M. Sastry, *J. Colloid Interface Sci.*, **275**, 496 (2004), https://doi.org/10.1016/j.jcis.2004.03.003
[44] M. R. Ahmadpour, M. Yousefi, H. Rakhshandeh, M. Darroudi, M. Mousavi *et al.*, *IEEE Trans. Nanobiosci.*, **23**, 118 (2024), https://doi.org/10.1109/TNB.2023.3287805
[45] H. Maqsood, M. Uroos, R. Muazzam, S. Naz and N. Muhammad, *Int. J. Biol. Macromol.*, **164**, 1847 (2020), https://doi.org/10.1016/j.ijbiomac.2020.08.073
[46] N. U. Rehman, G. Muhammad, M. Wajid, M. A. Hussain, T. Tuba *et al.*, *ChemistrySelect*, **10**, e02650 (2025), https://doi.org/10.1002/slct.202502650
[47] J. Zhang, T. Xing, A. F. El-kott, A. G. Alkhathami and A. A. Alamri, *J. Polym. Environ.*, **32**, 6495 (2024), https://doi.org/10.1007/s10924-024-03399-y
[48] C. Jayaseelan, R. Ramkumar, A. A. Rahuman and P. Perumal, *Ind. Crop. Prod.*, **45**, 423 (2013), https://doi.org/10.1016/j.indcrop.2012.12.019
[49] F. Iram, M. S. Iqbal, M. M. Athar, M. Z. Saeed, A. Yasmeen *et al.*, *Carbohyd. Polym.*, **104**, 29 (2014), https://doi.org/10.1016/j.carbpol.2014.01.002
[50] K. Adavallan and N. Krishnakumar, *Adv. Nat. Sci.: Nanosci. Nanotechnol.*, **5**, 025018 (2014), https://doi.org/10.1088/2043-6262/5/2/025018
[51] Y. Zhang, T. P. Shareena Dasari, H. Deng and H. Yu, *J. Environ. Sci. Health C*, **33**, 286 (2015)

[52] B. Abebe, H. C. A. Murthy and E. Amare, *J. Encapsul. Adsorpt. Sci.*, **8**, 225 (2018), https://doi.org/10.4236/jeas.2018.84012
[53] D. Zhu and Q. Zhou, *Environ. Nanotechnol. Monit. Manag.*, **12**, 100255 (2019)
[54] E. A. El-Sharkawy, A. Y. Soliman and K. M. Al-Amer, *J. Colloid Interface Sci.*, **310**, 498 (2007)
[55] S. Javed, M. R. Raza, M. U. Sharif, A. Majeed, M. A. Hussain *et al.*, *Desal. Water Treat.*, **318**, 100388 (2024), https://doi.org/10.1016/j.dwt.2024.100388
[56] G. K. Deokar and A. G. Ingale, *Inorg. Chem. Commun.*, **151**, 110649 (2023), https://doi.org/10.1016/j.inoche.2023.110649
[57] D. Baruah, M. Goswami, R. N. S. Yadav, A. Yadav and A. M. Das, *J. Photochem. Photobiol. B Biol.*, **186**, 51 (2018), https://doi.org/10.1016/j.jphotobiol.2018.07.002
[58] S. P. Pradhan, S. Swain, N. Sa, S. N. Pilla, A. Behera *et al.*, *Spectrochim. Acta A Mol. Biomol. Spectrosc.*, **282**, 121699 (2022), https://doi.org/10.1016/j.saa.2022.121699